Proton therapy

Proceedings Seventh NCS Lustrum Symposium

Amsterdam, the Netherlands, October 27, 2017

NEDERLANDSE COMMISSIE VOOR STRALINGSDOSIMETRIE

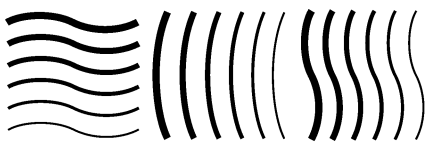

Netherlands Commission on Radiation Dosimetry

October 2017

Preface

The Nederlandse Commissie voor Stralingsdosimetrie (NCS, Netherlands Commission on Radiation Dosimetry, http://www.radiationdosimetry.org) was officially established on 3 September 1982 with the aim of promoting the appropriate use of dosimetry of ionising radiation both for scientific research and practical applications. The NCS is chaired by a board of scientists, installed upon the nomination of the supporting societies, including the Nederlandse Vereniging voor Radiotherapie en Oncologie (Netherlands Society for Radiotherapy and Oncology), the Nederlandse Vereniging voor Nucleaire Geneeskunde (Dutch Society of Nuclear Medicine), the Nederlandse Vereniging voor Klinische Fysica (Dutch Society for Medical Physics), the Nederlandse Vereniging voor Radiobiologie (Netherlands Radiobiological Society), the Nederlandse Vereniging voor Stralingshygiëne (Netherlands Society for Radiological Protection), the Nederlandse Vereniging voor Medische Beeldvorming en Radiotherapie (Dutch Society for Medical Imaging and Radiotherapy), the Nederlandse Vereniging van Klinisch Fysisch Medewerkers (Dutch Society for Medical Physics Engineers), the Nederlandse Vereniging voor Radiologie (Radiological Society of the Netherlands) and the Belgische Vereniging voor Ziekenhuisfysici/Société Belge des Physiciens des Hôpitaux (Belgian Hospital Physicists Association). To pursue its aims, the NCS accomplishes the following tasks: participation in dosimetry standardisation and promotion of dosimetry intercomparisons, drafting of dosimetry protocols, collection and evaluation of physical data related to dosimetry. Furthermore, the commission shall maintain or establish links with national and international organisations concerned with ionising radiation and promulgate information on new developments in the field of radiation dosimetry.

Proton therapy

Proceedings Seventh NCS Lustrum Symposium

Amsterdam, the Netherlands, October 27, 2017

NEDERLANDSE COMMISSIE VOOR STRALINGSDOSIMETRIE

Editors

Dr. N.A.P. Franken AMC, Amsterdam

Dr. J.B. van de Kamer NKI-AVL, Amsterdam

Dr. J.A. de Pooter VSL, Delft

Proton therapy

NCS, Delft, The Netherlands

For more information on NCS Reports, see http://www.radiationdosimetry.org

Table of Contents

Foreword

In 1982, the Nederlandse Commissie voor stralingsdosimetrie (NCS, Netherlands Commission on Radiation Dosimetry) was established, aiming to promote appropriate use of dosimetry of ionizing radiation, both for scientific and medical purposes. Over the last thirty years, the NCS has published twenty-seven reports, many concerning dosimetry in medicine. These reports have been highly appreciated in the field of radiation dosimetry in Belgium and the Netherlands, but also further abroad. Most reports serve as a Field Standard in the Netherlands and Belgium. The Board of the NCS aims to keep its reports up to date and relevant for professional users.

In close collaboration with the government and the supporting societies, the NCS platform has been given the chance to give input regarding the implementation of the European regulations to the Dutch Besluit basisveiligheidsnormen stralingshygiëne. In addition, a few NCS reports have been or will be published in periodicals of medical societies, such as PMB and phiRO. Such initiatives enlarge the exposure of the NCS activities which appears to be valued, given the steady increase in downloads of the various reports from the NCS website. Therefore, the board would like to thank all those volunteers participating in the NCS platform and the various NCS subcommittees.

The topic of today is “proton therapy” a subject that is becoming practical in Belgium and the Netherlands in the coming months. As we shall see today, proton therapy is a hot topic with many different aspects and new challenges. It is therefore no surprise that many of you have chosen to join us in this symposium.

We wish you all a pleasant and stimulating day.

On behalf of the NCS Board,

Jeroen van de Kamer

Overview proton therapy

M. van Vulpen

HollandPTC, Delft, The Netherlands

No abstract received.

Out-of-field radiation risks in paediatric proton therapy

C. Vandevoorde[1,2]

Department of Basic Medical Sciences, Ghent University

Beukes P[1], Miles X[1], Engelbrecht M[1], de Kock E[1], Symons J[1], Nieto-Camero J[1], Tran L[3], Lachlan C[3], Debrot E[3], Prokopovich, D[3,4] , Rosenfeld A[3], Chiriotti S[5], Parisi A[5], De Saint-Hubert M[5], Vanhavere F[5], Peterson S[6], Baeyens A[2], Vral A[2], Slabbert J[1].

[1] Radiation Biophysics Department, NRF iThemba LABS, South Africa

[2] Department of Basic Medical Sciences, Ghent University

[3] Centre for Medical Radiation Physics, University of Wollongong, Australia

[4] Australian Nuclear Science and Technology Organisation (ANSTO), South Africa

[5] Belgian Nuclear Research Centre (SCK-CEN), Belgium

[6] Department of Physics, University of Cape Town, South Africa

Background

The substantial increase in the clinical application of proton therapy (PT) over the last few year is attributable to the high degree of dose conformation and the lower integral whole-body dose of protons compared to conventional photon radiotherapy (RT), which result in a reduction of side effects. However, despite the dose sparing properties of protons, they do have the potential to produce unwanted dose outside the primary field due to stray radiation. Secondary particles, most importantly neutrons, are inevitably produced through nuclear interactions in the components of proton beam line and in patients' bodies. Current PT techniques are comprised of two main types: passive double-scattering proton therapy (DSPT) and pencil beam scanning proton therapy (PBS). Compared to DSPT, PBS reduces the dose to tissues upstream of the target and reduces the neutron dose in the patient caused by scattering devices and apertures in DSPT[1,2].

The stray radiation deposited outside the primary field may increase the risk of second malignancies. The latter is of particular importance for paediatric patients, known to be more radiosensitive and to have a longer life expectancy, which makes them especially susceptible to develop radiation-induced secondary cancer after RT[3]. Secondary neutron doses are very low (typically <0.1% of the target dose) and are thus negligible for treatment planning. However, low neutron doses have been well established to have a high biological

[1] Paganetti H (2011). Series in Medical Physics and Biomedical Engineering - Proton Therapy Physics (Boca Rato, FL; CRC)

[2] Cheng C, Moteabbed M, Xie Y, Schuemann J, Yock T, Paganetti H (2016). Assessing the radiation-induced second cancer risk in proton therapy for pediatric brain tumors: the impact of employing a patient-specific aperture in pencil beam scanning. Phys Med Biol 61; 12-22.

[3] Tukenova M, Guibout C, Hawkins M et al. (2011). Radiation therapy and late mortality from second sarcoma, carcinoma, and haematological malignancies after a solid cancer in childhood. Int J Radiat Oncol Biol Phys 80: 339-46.

effectiveness and potential for carcinogenesis[4]. For radiation protection purposes, radiation weighting factors (w_R) are used to convert the physical absorbed dose (Gy) into an equivalent dose (Sv)[5]. This concept is based on a simplified assumptions and there exists considerable uncertainty on how the relative biological effectiveness (RBE) for neutrons varies with dose and neutron energy, and whether the current RBE models and associated w_R are even appropriate for cancer risk estimation following PT. For the estimation of side effects from low out-of-field doses in PT, the quality factor concept based on the lineal energy transfer (LET), independent of the energy-depositing particle, could be more meaningful than the w_R formalism[6].

Given the existing large uncertainties, it is extremely important to quantify the neutron-related second cancer risk, in particular for paediatric patients. Previous studies measured and simulated the dose deposited outside the primary proton field by using a variety of techniques and detectors, however no radiobiological evaluation has been reported so far. The small doses and the fact that neutrons are uncharged particles make measurements and simulations challenging. Furthermore, the number of cases of second cancer following proton treatment to date is small, so poor statistics make epidemiological studies challenging.

Therefore, an interdisciplinary approach was used in this study, combining physics and radiobiology, to evaluate the out-of-field DNA damage attributable to stray radiation for paediatric DST applications. Although the most recent state-of-the-art PT facilities use PBS techniques, a large proportion of facilities worldwide is still based on passive scattering. Radiobiology measurements were supported by microdosimetry measurements to determine the relative contributions from neutron, gamma and scattered charged particle doses to the complete deposition of energy at specific out-of-field positions.

Methods

Whole blood samples (2.0 ml) from two donors were irradiated in test tubes at 6 locations in Perspex sleeves positioned in a water tank. In this study, we focussed a small affected volume, around 100mm from the field edge, simulating the head of a 5-y old child. Four fixed positions outside the primary proton field were used (A-10mm, B-35mm and E-60mm from the lateral field edge, all at 85mm depth and one downstream position C/D at 130mm depth), in addition to two reference positions in the field (at 30mm depth along the entrance plateau and at 85mm depth, which corresponds to the middle of the SOBP) (see Fig 1).

[4] NCRP. National council on radiation protection and measurements. The relative biological effectiveness of radiations of different quality. NCRP Report 104; 1990.

[5] ICRP (2007). The 2007 recommendations of the International Commission on Radiological Protection. ICRP Publication 103. Ann. ICRP 37 (2-4).

[6] Rossi H, Zaider M (1996). Microdosimetry and its applications (London, Springer).

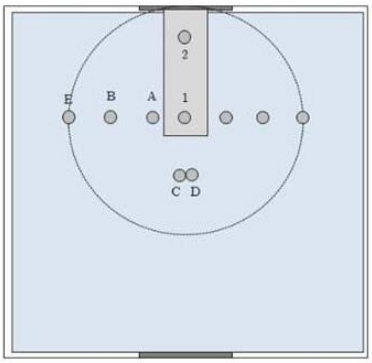

Figure 1: Diagram showing the positions of the different dosimeters and blood samples in the water phantom.

Dosimetric measurements were performed at the same positions with neutron bubble detectors (Bubble Technology Industries), Li6 and Li7 enriched thermoluminescent dosimeters (TLDs) and a silicon-on-insulator microdosimeter (MicroPlus^{TM} Probe). Irradiations were performed with a modulated clinical 200 MeV proton beam (range 100mm, collimator aperture 30mm and SOBP 31mm) and output factors (Gy/monitor unit) were measured with a T2 ionisation chamber. Whole blood samples were exposed to 0.2, 0.4, 0.6, 0.8 and 1 Gy doses at the six different positions and the micronucleus (MN) assay was performed to evaluate mutagenic effects of the out-of-field stray radiation. A first pilot Monte Carlo (MC) simulation was performed in Geant4. The code's basic setup is the proton accelerator at iThemba LABS, aimed at a water tank with a 31mm SOBP at 100mm range. The test tubes were modelled as 10 x 10 x 30mm cubes of water and the energy deposited was recorded. In order to reduce the errors on the small volumes, more particles will be run and the phantom will be better specified.

Results

Dose response curves for the out-of-field and reference positions were analysed and corresponding RBE values were calculated and will be presented. In addition, the results of the different dosimetric measurements will be presented, including microdosimetric spectra and y_D values for the different out-of-field positions. Dose Equivalent calculations based on quality factor and w_R conversion, will be critically evaluated and discussed in light of the measured neutron doses and RBE values for stray radiation in passive DSPT. These results are particularly important for paediatric patients, since the reduction of second cancer risk is in fact one of the principal reasons for the shift from photon-based therapy towards PT in paediatric oncology.

Acknowledgement

We wish to thank the Physics Advisory Committee (PAC) of NRF iThemba LABS for support and beam time allocation.

Reducing radiotherapy toxicity using protons: Insights from normal tissue radiobiology

P. van Luijk

Department Radiation Oncology, University Medical Centre Groningen, The Netherlands.

Radiotherapy plays an important role in the treatment of many tumours. However, dose administered to normal tissues surrounding the tumour frequently leads to side-effects. Therefore many technological developments of radiotherapy aim at reducing this dose.

The properties of the dose-depth profile of a proton beam offer new opportunities to reduce to normal tissues as compared to current photon-based techniques. In the region proximal to the Bragg peak, dose is reduced as compared to photons. In addition especially the lack of dose beyond the Bragg peak region offers enhanced planning flexibility. E.g. it facilitates choosing whether to spread normal tissue dose by using a large number of beams (a little to a lot), or to limit the involved volume by using a limited number of beams (a lot to a little). However, optimal use of such opportunities is poorly informed by clinical data available from photon-based treatments that lack these possibilities. To fill part of this gap, in vivo radiobiological studies have provided insight in mechanisms in and targets of the development of toxicity.

To this end high-precision proton irradiation of rats has been used to facilitate high-precision studies of volume effects and to elucidate the role of organ sub-structures in the development of radiation-induced failure of the parotid gland, lung and heart. A common finding in these organs is that organ failure depends strongly on the distribution of dose, rather than on metrics such as mean dose or irradiated volume.

Clinically sparing the parotid gland usually involves minimization of their mean doses. However, in our rat model the response of the parotid gland was found to depend on the region that was irradiated. Irradiation of the caudal 50% of the gland resulted in loss of at most 50% of the saliva production. In contrast, irradiation of the cranial 50% of the gland resulted in degradation of the whole gland and a disproportionate reduction of saliva production. This regional variation in response relates to the central localization of the parotid gland stem cells in the larger ducts. These cells are critical to long-term tissue homeostasis. Interestingly dose to this anatomical structure was also found to be the best predictor of post-radiotherapy saliva production in patients. Of relevance to proton therapy, we demonstrated that these cells are extremely sensitive to radiation. After ablating 50% of the gland, a dose of 1 Gy to the stem cell region was found to lead to an additional 20% loss of saliva production. This indicates that optimal sparing of the parotid gland may be achieved better with proton therapy than with IMRT, which is usually associated with extended volumes receiving a low dose.

In conclusion, in vivo radiobiology studies are critical to obtain insight in mechanisms of normal tissue damage critical to radiotherapy optimization.

Reference dosimetry in scanned proton beams

S. Rossomme[1] and C. Gomà[2,3]

[1]Molecular Imaging and Experimental Radiotherapy Department, Université Catholique de Louvain, Belgium

[2]KU Leuven, Department of Oncology, Laboratory of Experimental Radiotherapy, Leuven, Belgium

[3]UZ Leuven, Department of Radiation Oncology, Leuven, Belgium

Introduction and purpose

This talk covers the current status of reference dosimetry in scanned proton beams. The first part of the talk describes the current international recommendations, namely IAEA TRS-398 and ICRU Report 78, and their limitations when dealing with modern scanned proton beam delivery systems. Different possible routes to reference dosimetry of proton pencil beams are also described: absorbed dose to water at a point, dose-area product and Faraday cup dosimetry. In the second part, we review the most recent key data in proton dosimetry: ion recombination correction factor (k_s) and beam quality correction factors (k_Q).

Materials and methods

Beam quality correction factors

Monte Carlo calculation

Very few Monte Carlo calculated k_Q data have been published for scanned proton beams. The main reason being that most Monte Carlo codes with validated proton transport do not allow for a detailed simulation of electron transport—crucial for an accurate simulation of detector response. Gomà *et al* (2016) calculated k_Q factors in scanned proton beams for plane-parallel and few cylindrical ionization chambers using PENH. Sorriaux *et al* (2017) calculated f_Q factors in modulated-scanned and modulated-scattered beams for a plane-parallel and a cylindrical chamber using GATE-Geant4.

Calorimetry

A calorimeter is considered a primary standard for absorbed dose, because it allows a direct measurement of the total energy absorbed per unit mass. The principle of calorimetry is to measure the temperature rise in a medium due to energy absorbed from the radiation beam and multiply this temperature rise by the specific heat capacity of the medium. Although its basic principle of operation is simple, a calorimetry procedure is time-consuming and complex since it requires a large number of measurements and a range of corrections that require different numerical analyses approaches for modelling physical and chemical process. For these reasons there are few calorimeters in the world and they are mainly confined to primary standards laboratories, such as LNHB (France), NRC (Canada), NPL (UK), PTB (Germany) or VSL (The Netherlands). In the academic sector, some researchers at McGill University (Canada), Lund University (Sweden) and Université catholique de Louvain (Belgium) developed and used calorimeters. There are mainly two types of calorimeters: graphite and water calorimeters. The advantage of a water calorimeter is that it determines absorbed dose to water directly from its definition. Using a graphite calorimeter, a

dose conversion depending on water to graphite electronic mass stopping power ratio and fluence correction factor is needed, which introduces an additional uncertainty. At present, no primary standard for absorbed dose-to-water exists for proton beams. A first dedicated portable graphite calorimeter for proton and light-ion radiotherapy beams has recently been built at NPL.

To derive experimental k_Q-factors from calorimetry, a direct comparison of the absorbed dose determined by a calorimeter and ionization chambers must be performed. As recommended by international dosimetry protocols, classical correction factors have to be applied to the response of ionization chambers: temperature and pressure, polarity and recombination.

Ion recombination correction factor

As recommended by TRS-398 and ICRU 78, an ion recombination correction factor has to be applied to the response of ionization chambers. Two contributing processes are distinguished: initial and volume recombination. Initial recombination occurs between ions created within the same track and depends on the ionization density within the track. Volume recombination takes place between ions originating from different tracks and depends on the dose rate. Numerous theories have been published to describe both mechanisms, such as the theories of Jaffé, Kara-Michailova or Onsager for initial recombination and the theories of Boag, Greening and Mie for volume recombination.

Results and discussion

Beam quality correction factor

Monte Carlo calculation

Gomà et al (2016) reported that, for plane-parallel ionization chambers, Monte Carlo calculated k_Q factors agreed with the theoretical values tabulated in IAEA TRS-398. For cylindrical chambers, however, differences up to 1.8% with respect to TRS-398 were reported, but good agreement with the scarce water calorimetry data published to that date. Recently Sorriaux et al (2017) showed that k_Q factors in modulated-scanned proton beams are consistent with those in modulated-scattered beams.

Calorimetry

Many works have been performed concerning the use of calorimetry in conventional beams (photon and electron beams). In proton beams, the publications are less numerous, but the existing conclusions given by Palmans et al (2004), Sarfehnia et al (2010) and Medin (2010) are positive. Palmans et al (2004) reported a comparison between the response of ionization chambers and the response of a graphite calorimetry data in passive ocular proton beams. Depending on the beam type (mono-energetic beam or modulated beam) and the ionization chamber calibration beam (Cobalt-60 or electron beam), the ratio between both detectors varied between 0.983 and 1.019, with a standard uncertainties between 1.9% and 2.5%. Sarfehnia et al (2010) demonstrated the feasibility of using a water calorimeter in a scanned proton beam. Comparing the response of a water calorimeter and the response of ionization chambers in a 180 MeV scanned pulsed proton beam, Medin (2010) determined experimental k_Q factors for two NE2571 Farmer chambers. The experimental k_Q factors was found to be 1.032 ± 0.013, which is in good agreement with the factor tabulated in IAEA TRS-398 for this chamber type (1.039 ± 0.018). Recently, experimental works have been

performed in pulsed pencil beam scanning (PBS) proton beams by Rossomme et al. Preliminary results show the feasibility of using a water calorimeter in such beams.

Ion recombination correction factor

Currently, questions about the impact of the PBS technique (pulsed or not) on the response of the ionization chambers, in particular about ion recombination mechanism, are investigated. Few data have been published. Figure 1 shows experimental ion recombination correction factors as a function of the inverse of the polarising voltage obtained using a clinical dose rate. Results obtained using a plane-parallel chamber (IBA PPC40 or PTW Roos) and a cylindrical ionization chamber (NE2571) are represented in blue and black, respectively. Figure 1 shows data obtained in a 60 MeV passive proton beam, a 100 MeV PBS proton beam and a 96 MeV pulsed PBS proton beam, respectively.

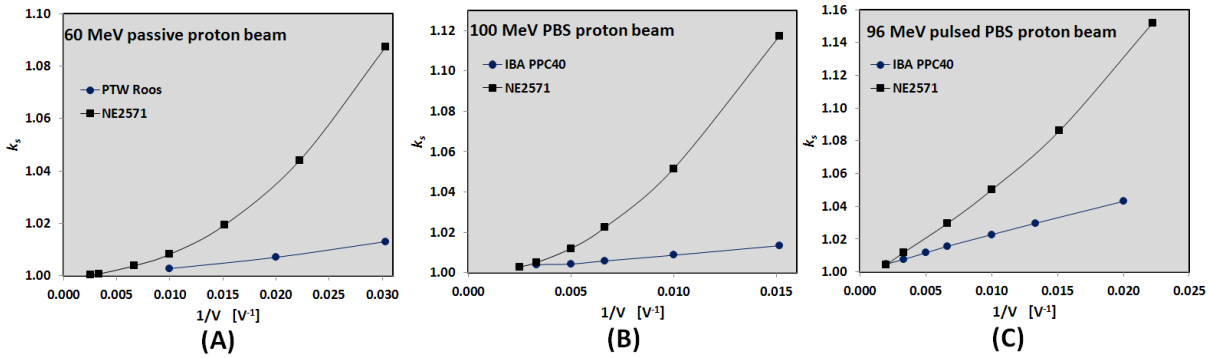

Figure 1. Ion recombination correction factors as a function of the inverse of the polarising voltage (1/V) obtained for a plane-parallel ionization chamber (blue) and a cylindrical chamber (black), in three different proton beams.

For plane-parallel ionization chambers, in passive and pulsed PBS proton beams, Palmans et al (2006) and Rossomme et al (2017) reported an excellent agreement between experimental data and models combining two theories: Jaffé's theory (logarithmic variation of initial recombination contribution as a function of 1/V, which can be approximated, in first order, by a linear function of 1/V) and Boag's theory (variation of volume recombination contribution as a function of 1/V or 1/V² - in first order). Although initial recombination has a small influence on the ion recombination correction factors, due to the low LET value of proton beams, it is important to take them into account. For PBS proton beams, results are under investigations.

For cylindrical ionization chambers, due to the large volume of the air cavity, ion recombination correction factors are larger than those obtained using a Roos-type ionization chamber. Results are under investigations to compare experimental results with theoretical models.

Conclusions

Current international dosimetry protocols (IAEA TRS-398) should be applied carefully to scanned proton beams, especially when it comes to low-energy proton beams.

The scarce Monte Carlo and calorimetry data on k_Q factors seems to agree with the theoretical values tabulated in IAEA TRS-398, within their large standard uncertainty (2%).

Concerning ion recombination, experimental results confirm that ion recombination correction factors cannot be neglected in clinical pulsed PBS proton beams. The solution to minimise k_s–values and its fluctuation resulting from the dose rate variations is to use the ionization chamber at high voltage. However, in that case one has to account with charge multiplication in the ionization chamber.

References

Gomà *et al* (2016) Phys Med Biol 61(6):2389-2406

Medin (2010) Phys Med Biol 55(12):3287-98

Palmans *et al* (2004) Phys Med Biol 49(16):3737-49

Palmans *et al* (2006) Phys Med Biol 51(4):903-17

Rossomme *et al* (2017) Phys Med Biol 62(13):5365-5382

Sarfehnia *et al* (2010) Med Phys 37(7):6381-93

Sorriaux *et al* (2017) Med Phys. doi: 10.1002/mp.12434

Dual-energy CT for proton therapy

I. Almeida

Maastro Clinic, Maastricht, The Netherlands

Computed tomography (CT) imaging gives the photon linear attenuation of the scanned object expressed in Hounsfield Units (HU). The HU of a given material depend on the energy and the filtration of the x-ray tube. A scanner specific calibration for each protocol is needed to convert the CT image to mass densities or, in proton therapy, to stopping power ratios (SPR).

Dual-energy computed tomography (DECT) imaging has the potential to improve tissue characterization by adding a second set of data to the same scanned material at a different energy, enabling the calculation of the tissue's relative electron density (RED) and effective atomic number (EAN). These two quantities are used to calculate the SPR and to perform tissue segmentation.

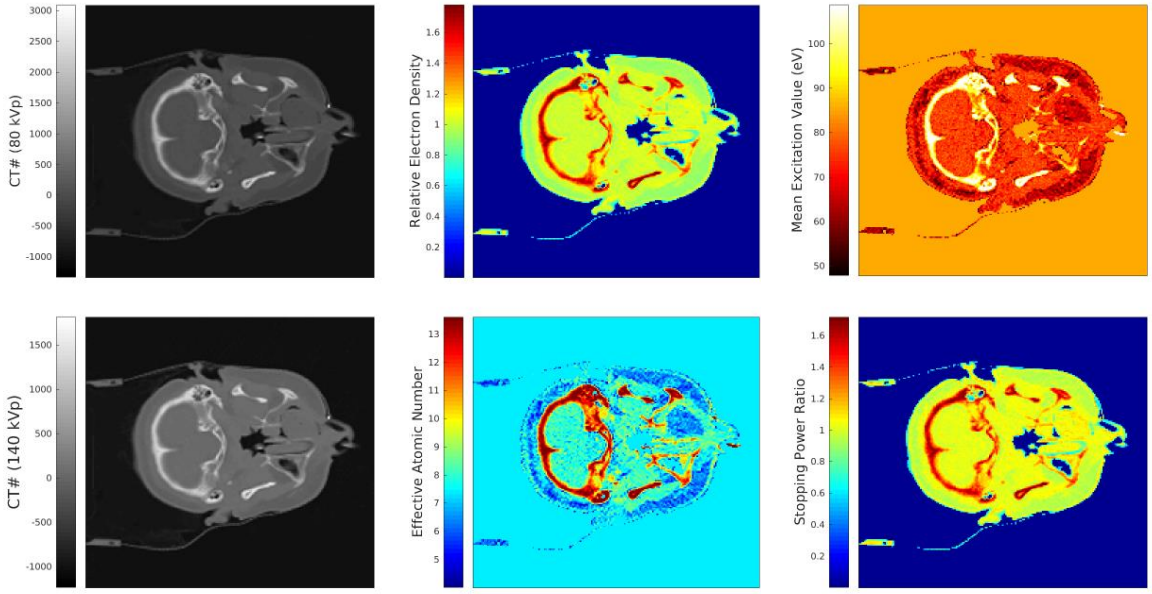

Figure 1. Images of a H&N patient: DECT scans at 80 kVp and 140 kVp (left column), RED and EAN images (middle column) and I-value image and SPR-map for 100 MeV protons (right column).

Different approaches are being studied to perform dose calculations based on DECT, either by giving directly the SPR map or providing the materials and densities of the voxelized geometry. This talk will present the DECT methodology, cover recent publications that show higher accuracy in range determination from using DECT for proton treatment planning instead of the conventional CT, as well as present the questions and technical limitations that still need to be address.

Relative dosimetry for scanned pencil beam proton therapy

P. Trnková

HollandPTC, Delft & Erasmus MC, Rotterdam, The Netherlands

Introduction

A proton pencil beam is characterized by integral depth dose curves (IDDs) and angular and spatial distribution, so called phase space. Together with beam monitor calibration are these characteristics an essential input for the dose calculation engines in the treatment planning systems (TPSs) for pencil beam scanned (PBS) proton therapy [1, 2]. In this talk, an overview about currently used methods to measure IDDs and characterize phase space will be presented. The talk summarizes an international practice.

Integral depth dose curves (IDDs)

The proton energies usually used clinically are approximately from 70 MeV up to 240 MeV corresponding to the ranges of 4 g / cm^2 to 36 g / cm^2, respectively. The selection of other energies between the minimal and maximal energy available in a given system is used to create a uniform spread out Bragg peak (SOBP) using a scanning beam with a superposition of pristine Bragg peaks [3]. During the commissioning, IDDs for a representative set of energies are measured and the rest of the clinically used energies is interpolated.

The measurements are performed with large plane parallel ionization chamber (IC), so called Bragg peak chamber. Due to the multiple Coulomb scattering (MCS), the protons traversing a matter are deflected in many small angles leading to loss of the fluence along the central beam axis [4]. Therefore, it is important to use large IC to capture the whole proton beam.

Currently commercially available Bragg peak chambers have a diameter between 8 to 12 cm. This diameter is, however, not sufficient to detect the whole proton beam for higher energies. As the range of the higher energy protons is longer the scattering of the primary proton beam is broader [5] leading to (small) fraction of dose being deposited outside the detection volume [6]. The missing fraction of the dose must be precisely estimated either by Monte Carlo simulation [4], Golden beam data approach [6] or analytical models [7] and the measured IDDs must be corrected.

Increasing the size of the Bragg peak chamber might be a possible solution to overcome the problems with MCS but it is difficult to state what size would be sufficient enough. The size of the chamber would depend on the initial size of the proton beam (facility specific) and amount of dose accepted to be deposited outside of the chamber. Moreover, for a very large chamber, characteristics such as a position stability in a water tank, radial linearity and energy dependence of the dose response would be a big challenge.

It is worth mentioning, that large electrode multilayer ionization chambers (MLICs) have been developed and are often used for IDDs measurements [8]. This device contains up to 200 Bragg peak chambers (depending on the manufacturer) positioned one after the other and enables simultaneous measurement in all the chambers providing extremely fast measurement of IDDs. The measurement is not performed in water and a linear function is

used to relate the position of MLIC channels to the depth in water. Because of that, the acquired IDDs should not be used as input data for a TPS.

Angular and spatial dose distribution

Due to the beam optics and accelerator characteristics, the in-air size and shape of an individual pencil beam varies depending on the energy, distance from the isocenter and divergence of the beam [3]. The size of a pencil beam can differ from a couple of mm up to few cm. Its Gaussian shape is not perfectly circular nor symmetrical and must be therefore characterized in both scanning directions across a transverse plane.

Typically, measurements to map the whole phase space are performed for a set of energies, usually the same ones that were used for IDDs measurements, at several distances from nozzle. As the beam optics focuses the beam into the isocenter, i.e. smallest pencil is at the isocenter, the pencil beam size will be slightly bigger off the isocenter [9].

In order to obtain a measurement with sub-millimeter accuracy, a detector with high spatial resolution perpendicular to the beam direction is required. A two-dimensional plastic scintillating screen in a combination with a 45° mirror and a charge-coupled device (CCD) camera are most commonly used [2]. Such a device enables a quick measurement with online evaluation. Their big disadvantage is the high dependence of the output of plastic scintillating materials the linear energy transfer (LET) and thus the light output is not proportional to the energy deposited in the scintillator. This effect is called quenching and it is a main reason why scintillation screens can be used only for relative measurements [10].

For a single energy, the response of a scintillator is linear, i.e. the light output is proportional to the beam intensity. However, plastic scintillators are known to show light output saturation when the dose is large.

These measurements can be also performed with radiochromic films [1]. The same issues, like quenching and saturation will be present. Moreover, the evaluation times will be significantly longer as no online evaluation is possible. A flat panel detector based on amorphous silicon is currently investigated by several centers to evaluate whether it can be a possible alternative to scintillation screens and radiochromic films for phase space measurements [11].

Conclusion

An overview of currently available methods for relative dosimetry was provided. These methods will be part of the recommendations for the Benelux proton therapy centers and will be summarized in the future NCS report.

References

[1] Gillin MT, Sahoo N, Bues M, Ciangaru G, Sawakuchi G, Poenisch F, et al: *Commissioning of the discrete spot scanning proton beam delivery system at the University of Texas M.D. Anderson Cancer Center, Proton Therapy Center, Houston*; Med Phys 2010, 37(1): 154-63

[2] Langner UW, Eley JG, Dong L, Langen K: *Comparison of multi-institutional Varian ProBeam pencil beam scanning proton beam commissioning data*; J Appl Clin Med Phys 2017, 18(3): 96-107

[3] Das IJ, Paganetti H: *Principles and practice of proton beam therapy*; Medical Physics Publishing, Inc., Medison, Wisconsin, 2015

[4] Fippel M, Soukup M: *A Monte Carlo dose calculation algorithm for proton therapy*; Med Phys 2004, 31(8): 2263-73.

[5] Gottschalk B, Cascio EW, Daartz J, Wagner MS: *On the nuclear halo of a proton pencil beam stopping in water*; Phys Med Biol 2015, 60(14): 5627-54

[6] Clasie B, Depauw N, Fransen M, Gomà C, Panahandeh HR, Seco J, Flanz JB, Kooy HM*: Golden beam data for proton pencil-beam scanning*; Phys Med Biol 2012, 57(5): 1147-58

[7] Pedroni E, Scheib S, Böhringer T, Coray A, Grossmann M, Lin S, Lomax A: *Experimental characterization and physical modelling of the dose distribution of scanned proton pencil beams*; Phys Med Biol 2005, 50(3): 541-61.

[8] Bäumer C, Koska B, Lambert J, Timmermann B, Mertens T, Takoukam Talla P: *Evaluation of detectors for acquisition of pristine depth-dose curves in pencil beam scanning*; J Appl Clin Med Phys 2015, 16(6): 5577

[9] Safai S, Bortfeld T, Engelsman M: Comparison between the lateral penumbra of a collimated double-scattered beam and uncollimated scanning beam in proton radiotherapy; Phys Med Biol 2008, 53(6): 1729-50

[10] Safai S, Lin S, Pedroni E: *Development of an inorganic scintillating mixture for proton beam verification dosimetry*; Phys Med Biol 2004, 49(19): 4637-55

[11]Hartmann B, Telsemeyer J, Huber L, Ackermann B, Jäkel O, Martišíková M: Investigations of a flat-panel detector for quality assurance measurements in ion beam therapy; Phys Med Biol 2012, 57(1): 51-68

MR-guided proton therapy: current status and beyond

A.L. Hoffmann

OncoRay - National Center for Radiation Research in Oncology, Dresden, Germany

Imaging plays an important role in the treatment planning and dose delivery phase of today's radiation therapy practice. However, its role during proton beam dose delivery has thus far been limited. Currently, in-room image guidance is mainly based on orthogonal X-ray imaging and only in some centers in-room CT or cone-beam CT imaging is available. While the latter two are expected to reduce geometric uncertainties resulting from inter-fractional changes in patient anatomy and treatment setup, they provide poor soft-tissue contrast and have limited capabilities for intra-fractional real-time imaging.

Precise coverage of the target volume in proton therapy is even more challenging than in conventional (photon) radiotherapy, because protons are more sensitive to anatomical variations (*e.g.*, organ motion and deformation) and patient set-up inaccuracies. This is due to the steep dose fall-off behind the Bragg peak and to the fact that the range of the proton beam strongly depends on the material composition in the beam path. These uncertainties currently translate into relatively large safety margins, thus compromising the dosimetric benefit of proton therapy. This urges the need for real-time 3D image guidance during proton beam delivery, which can be offered by magnetic resonance imaging (MRI).

MRI should, therefore, have a higher potential for improving precision for particle than for photon therapy. However, a number of hitherto open technological questions have to be carefully studied and solved before MR-guided proton therapy (MRgPT) can be clinically implemented. These open questions are in particular:

1. Lorenz-force induced energy-dependent bending of the proton beam in the magnetic field of an MRI scanner and accordingly a distortion of the dose distribution, which has to be quantified and taken into account in treatment planning.
2. MRgPT requires the operation of an MRI scanner in an environment contaminated by a transient electromagnetic field of at least two origins: a) The accelerating voltage of particle accelerators with typical radiofrequencies between 10-100 MHz, and b) magnetic fields for guiding the therapy beam change with typical time constants between milliseconds and seconds. To compensate for the influence of this electromagnetic interference on MR image quality new shielding measures and image acquisition schemes may be necessary and have to be investigated and implemented.
3. The magnetic field of an MRI scanner will interact with detectors for clinical dosimetry and can compromise the results of such measurements. Consequently, proton radiation detectors for application in magnetic fields have to be selected, evaluated or even developed. Furthermore, the quality assurance procedures of proton therapy in the presence of strong magnetic fields have to be established. Solving these questions is indispensable for a development towards MRgPT.
4. For on-line (adaptive) treatment planning, the dose deposition along the proton beam path needs to be calculated from real-time MR images, requiring a fast translation of MR image information into electron density or electronic stopping power. Such methods do not yet exist and hence need to be developed.

Dosimetric effects of proton beams in the presence of magnetic fields

Various groups have performed simulation studies on the feasibility of some aspects of MRgPT. Studies have looked at the fundamental beam transport and dosimetry changes, in particular the magnitude of the deflection of proton beams by strong magnetic field typically found in the imaging volume of an MRI scanner. These include estimation of the beam deflection inside a water phantom by Raaymakers *et al*. [1], Wolf and Bortfeld [2], Fuchs *et al*. [3] and Schellhammer and Hoffmann [4]. Optimised patient-based treatment planning in uniform magnetic fields to account for the beam deflection has been studied by Motteabbed *et al*. [5] and Hartman *et al*. [6]. These studies assumed a static external magnetic field without fringe field effects of the MRI scanner. Oborn *et al*. [7] showed that the fringe field of an MRI scanner has a complex and significant impact on how a proton beam transports towards the magnetic isocentre of an MRI scanner. An important implication of this work is that the most reliable method for dose delivery in MRgPT will be with the pencil beam scanning method. Passively scattered beams, which contain a broad energy range, will deflect and distort in a complex way as they travel through the spatially variant fringe field, whereas the pencil beam scanning method will require simple spatial correction on a per-pencil beam basis in order to achieve the correct Bragg peak locations for each pencil beam [4].

So far, the dosimetric effects of proton beams in magnetic field reported in literature have been studied by simulations. Experimental evidence on the accuracy of proton beam dose calculation methods in a realistic magnetic field has been lacking. Recently, our group for the first time showed dosimetric proof-of-principle with proton pencil beams of 80−180 MeV begin stopped in a tissue-mimicking slab phantom being placed inside the transversal magnetic field of a 0.95 T permanent NdFeB dipole magnet assembly [8]. Proton beam trajectories and depth-dose curves in the presence of the magnetic field were measured with Gafchromic EBT3 film, being placed parallel to the beam direction amidst two slabs of the phantom, and compared against Monte Carlo simulations. The results show good agreement, and indicate that magnetic field induced beam deflection is measurable and accurately predictable (Figures 1−3). This demonstrates the feasibility of accurate dose calculation for a proton pencil beam in a magnetic field, and facilitates the treatment planning thereof.

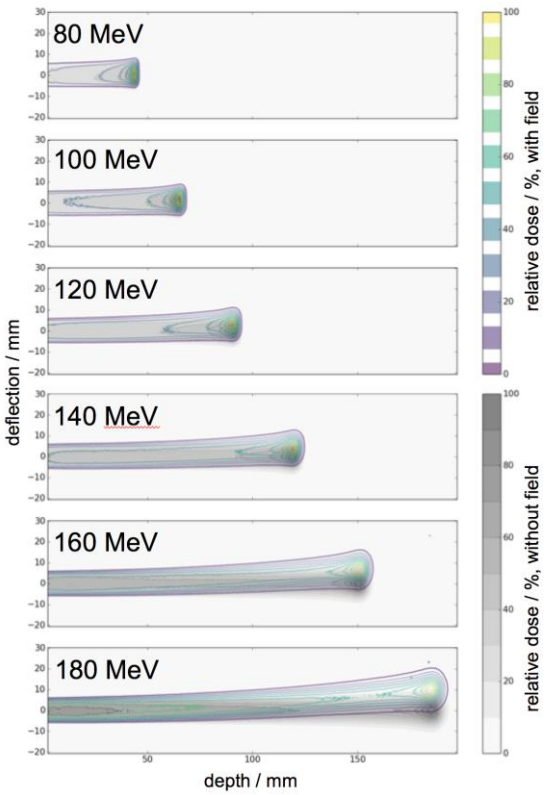

Figure 1. Measured relative dose distributions of 80–180 MeV proton pencil beams in PMMA without (grey scale) and with (color coded) magnetic field.

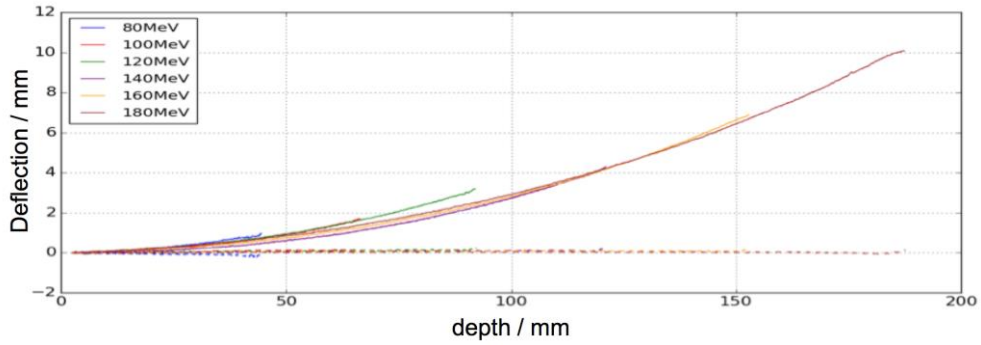

Figure 2. Measured proton beam trajectories in PMMA with (solid lines) and without (dashed lines) magnetic field.

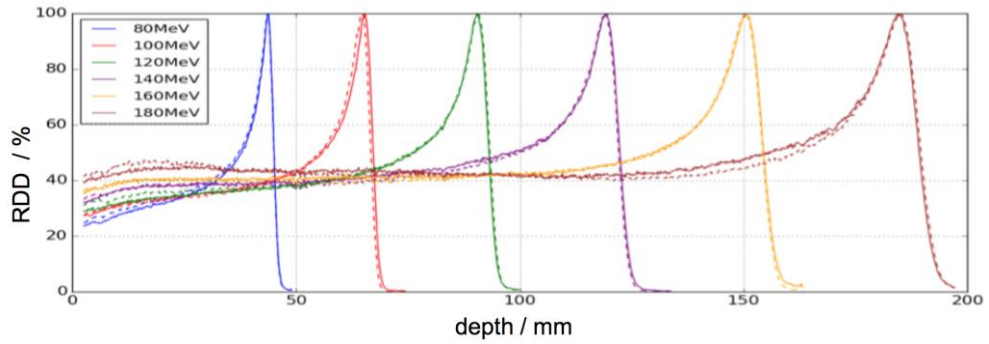

Figure 3. Measured relative depth-dose curves in PMMA with (solid lines) and without (dashed lines) magnetic field.

Mutual electromagnetic interaction between proton therapy system and MRI system

As noted by Schippers and Lomax [9], a challenging aspect of integrating MRI and proton therapy is the compensation of the mutual influence of the proton beamline transport magnets on the magnetic field of the MRI scanner, as well as magnetic field effects on beam control and monitoring systems.

Data on the mutual interference of these two systems is very scarce in literature, and MRI scanner manufacturers typically do not specify the site requirements to operate an MRI scanner in the vicinity of a cyclotron, beamline or rotating gantry. Cheng *et al*. [10] recently published the first report on the interference of a strong time-varying magnetic field and the RF power of a state-of-the art compact proton therapy system in a nearby MRI facility. They showed that with careful site planning on RF shielding and elaborate measurements on the RF and magnetic field effects, the MRI system's performance was not compromised during operation of the proton therapy system. However, installing the MRI scanner inside the treatment room or even trying to integrate it with the gantry for isocentric imaging will dramatically increase the complexity and raise the technical challenges to meet the magnetic field and RF constraints for both the MRI system and the proton therapy system to operate without mutual interference.

Proton beam dosimetry in the presence of magnetic fields

The magnetic field impacts the response of dosimetry equipment used to characterize proton beams. Effects of magnetic field exposure on different types of dosimetry tools used for quality assurance of proton therapy should be investigated when implementing them in the context of MRgPT. Currently, no QA procedures of proton therapy in the presence of strong magnetic fields have been established.

To this end, knowledge on dedicated radiation dosimetry methods and procedures developed for linear accelerator units integrating conventional photon therapy and MRI (*e.g.* ViewRay MRIdian® and Elekta Unity systems) could be instrumental.

For two-dimensional high-resolution dosimetry of un-modulated proton beams, Gafchromic EBT films are often used as a time-efficient method to obtain the depth-dose curve and beam range in a single measurement [11]. As recently shown by Reynoso *et al*. [12] for ^{60}Co γ-rays of the ViewRay MRIdian® system, using Gafchromic EBT2 film in a magnetic field may affect monomer crystal orientation and polymerization within its active layer. Their results suggest that magnetokinetic changes may be the dominant factor for the observed dose-dependent

under-response of this film in the presence of a magnetic field. A complete characterization and study of the magnetic field effects of the newer EBT3 film for proton beams is ongoing in our group.

MR-only based treatment planning

Electronic stopping power is the most important tissue property influencing proton dose distributions. Currently, a CT-based conversion of electronic density (*i.e.* Hounsfield units) into stopping power ratios is exploited for proton treatment planning. Since MR images do not contain electron density information, they cannot be directly used for radiation treatment planning.

The feasibility of MRI-only based planning for proton therapy has been investigated previously by Rank *et al*. [13,14] and Edmund *et al*. [15] using different classification-based tissue segmentation methods to generate so-called pseudo-CT images from MR images. Both employed ultrashort echo time MRI sequences for patients with brain tumours. Although issues arose related to bone and air identification, the dose distributions of the proton therapy plans showed only minor or clinically acceptable deviations from those obtained by the reference CT images. Recently, Koivula *et al*. [16] generated pseudo-CT images of patients with brain and prostate cancers by transforming the intensity values of in-phase MR images into Hounsfield units, and showed a gamma index criterion for the proton dose distributions over 91% at the 1%/1mm tolerance level.

For more heterogeneous tissues, various studies have pointed out relatively large uncertainties in the stopping power ratios for protons used in the dose computation. Furthermore, classification-based tissue segmentation methods are too slow to be employed for treating moving targets. Hence, a more accurate and fast translation of MR image information into electronic stopping power is required. The use of dedicated MRI sequences to establish the water-equivalent path length of protons in heterogeneous tissues is currently under investigation.

Summary and outlook

Current knowledge supports the feasibility of MRgPT only from a phantom and patient dosimetry point of view. Good progress has been made for MR-only based treatment planning on static target volumes, but there is a clear need for further development towards application for moving target volumes. Methods and procedures for proton beam dosimetry in the presence of magnetic fields need to be established. Currently, there are no studies addressing fundamental questions such as the operation of an in-room MRI scanner in the presence of a proton beam delivery system or the specific design requirements for future MRgPT prototype equipment. As recently noted by Oborn *et al*. [17] the steps required to bring this yet unreleased advanced technology forward comprise of:

1. Software for robust treatment planning and guidance with real-time MR images specific to proton therapy.
2. Hardware for new gantry designs and beam delivery verification methods.

Clearly, the latest technological milestone in image-guided radiation therapy (IGRT) is the integration of real-time MRI systems and linear accelerators for conventional photon therapy. By integrating real-time MRI and proton therapy both the dosimetric quality and potential clinical superiority of the latter over existing photon-based IGRT treatments are expected to

improve significantly. The promising results obtained so far urge to further explore the feasibility and capabilities of MRgPT.

References

[1] Raaymakers BW, Raaijmakers AJ, Lagendijk JJ. Feasibility of MRI guided proton therapy: magnetic field dose effects. *Phys Med Biology*, 53(20): 5615–5622, 2008.

[2] Wolf R, Bortfeld T. An analytical solution to proton Bragg peak deflection in a magnetic field. *Phys Med Biol*, 57(17): N329–N337, 2012.

[3] Fuchs H, Moser P, Gröschl M, Georg D. Magnetic field effects on particle beams and their implications for dose calculation in MR-guided particle therapy. *Med Phys*, 44(3): 1149–1156, 2017.

[4] Schellhammer SM, Hoffmann AL. Prediction and compensation of magnetic beam deflection in MR-integrated proton therapy: a method optimized regarding accuracy, versatility and speed. *Phys Med Biol*, 62(4): 1548–1654, 2017.

[5] Motteabbed M, Schuemann J, Paganetti H. Dosimetric feasibility of real-time MRi-guided proton therapy. *Med Phys*, 41(11): 111713, 2014.

[6] Hartman J, Kontaxis C, Bol GH, Frank SJ, Lagendijk JJ, van Vulpen M, Raaymakers BW. Dosimetric feasibility of intensity modulated proton therapy in a transverse magnetic field of 1.5 T. *Phys Med Biol*, 60(15): 5955–5969, 2015.

[7] Oborn BM, Dowdell S, Metcalfe PE, Crozier S, Mohan R, Keall P. Proton beam deflection in MRI fields: Implications for MRI-guided proton therapy. *Med Phys*, 42(5): 2113–2124, 2015.

[8] Lühr A, Gantz S, Schellhammer S, Zarini O, Zeil K, Schramm U, Hoffmann A. In-magnet measurement setup for proof-of-concept and commissioning of MR integrated proton therapy. *Radiother Oncol*, 124(Suppl 1): S221–222, 2013.

[9] Schippers JM, Lomax AJ. Emerging technologies in proton therapy. *Acta Oncol*, 50(6): 838–850, 2011.

[10] Cheng CW, Ferguson SG, Jordan D, Jesseph F, Johnson M, Bouchet L, Mansur D, Wessels B. Impact of the high magnetic field and RF power in a superconducting cyclotron on the operation of a nearby MRI facility. *Jour Proton Ther*, 2(1): 213–223, 2016.

[11] Zhao L, Das IJ. Gafchromic EBT film dosimetry in proton beams. *Phys Med Biol*, 55(10): N291–301, 2010.

[12] Reynoso FJ, Curcuru A, Green O, Mutic S, Das IJ, Santanam L. Technical Note: Magnetic field effects on Gafchromic-film response in MR-IGRT. *Med Phys*, 43(12): 6552–6556, 2016.

[13] Rank CM, Hünemohr N, Nagel AM, Röthke MC, Jäkel O, Greilich S. MRI-based simulation of treatment plans for ion therapy in the brain region. *Radiother Oncol*, 109(3): 414–418, 2013.

[14] Rank CM, Tremmel C, Hünemohr N, Nagel AM, Jäkel O, Greilich S. MRI-based treatment plan simulation and adaptation for ion therapy using a classification-based approach. *Radiat Oncol*, 8: 51, 2013.

[15] Edmund JM, Kjer HM, van Leemput K, Hansen RH, Andersen JA, Andreasen D. A voxel-based investigation for MRI-only radiotherapy of the brain using ultra short echo times. *Radiat Oncol*, 8: 51, 2013.

[16] Koivula L, Wee L, Korhonen J. Feasibility of MRI-only treatment planning for proton therapy in brain and prostate cancers: Dose calculation accuracy in substitute CT images. *Med Phys*, 43(8): 4634–4642, 2016.

[17] Oborn BM, Dowdell S, Metcalfe PE, Crozier S, Mohan R, Keall P. Future of medical physics: Real-time MRI-guided proton therapy. *Med Phys*, 42(5): 2113–2124, 2015.

Clinical application of proton beam therapy

C. Rasch

Department of Radiation Oncology, AMC, Amsterdam, The Netherlands

No abstract received

Radiation protection in a proton therapy centre

Pieternel van der Tol[1]

HollandPTC, Delft, The Netherlands

Introduction

Proton beam cancer therapy uses medical cyclotrons accelerating protons to high energies of up to 250 MeV, with proton currents in the order of hundreds of nA [1]. In the Netherlands three proton therapy centers are being built. Like conventional photon and electron radiotherapy, proton therapy comes with its own particular challenges in radiation protection. This talk will highlight important radiation safety issues related to proton therapy, and focus on the occupational exposure and possible strategies to mitigate the risks.

Proton interactions

The interaction of high energy protons with matter will result in a complex field of secondary radiation. This secondary radiation field is the main source for radiation safety issues, as the proton beam itself usually stops in the patient, and therefore does not reach personnel. Proton-matter interactions can be divided into three main interactions types. First, the stopping of protons in matter is mostly a result of electromagnetic interactions. These interactions lead to secondary electrons and X-ray photons. Second, protons have elastic interactions with nuclei, leading to a change in proton trajectory and thus scattering of the proton beam. Third, inelastic nuclear interactions between the proton and nuclei in a target material can result in secondary neutrons, electrons, protons, deuterons, tritium, α particles and other ions, as well as gamma photons [2].

The yield, energy and type of secondary radiation depends on both the proton energy and the target material. The highest energy secondary particles are produced by nuclear interactions or cascades. For example, neutrons produced by this type of interaction can have energies close to the primary proton energy [2]. Neutrons produced in proton therapy pose a potential risk to staff, as they can be extremely penetrating and have a high relative biologic effectiveness (RBE). The RBE is dependent on the energy of the neutrons, and can be as high as 20 for 1 MeV neutrons. For the typical secondary spectrum of neutrons generated in proton therapy, the average RBE is 7 (i.e. will produce seven times the damage caused by an equal amount of energy absorbed as photons) [3].

Secondary radiation will disappear once the proton beam is turned off. However, the nuclear interactions of high energy protons can result in unstable residual fragments, that will eventually decay to a stable form. These fragments usually remain in the material, that should in turn be treated as a radioactive material. This process is known as activation. In addition, secondary neutrons are also a main cause of activation of materials. Activation can occur in materials in cyclotron and beamline, shielding, and in the gantry room: range shifters, apertures, patients and air can all be activated [4].

Mitigation of risks

Occupational exposure in proton therapy can be as low as 1.5 mSv for radiation therapy technologists [5]. The radiation exposure to staff and members of the public is limited by a combination of structural design, monitoring, and safety culture and strict administrative controls.

Shielding design of a proton therapy facility is a complex task, that mainly focusses on the shielding of secondary neutrons, as they will require the most shielding. This is similar to shielding design for conventional radiotherapy, with the main differences being that the secondary neutrons can have a much higher energy and the installation that needs to be shielded is usually larger (i.e. cyclotron, beamline, gantry rooms). Typically, several meters of concrete are chosen as a shielding material.
Two approaches to calculate the necessary shielding are commonly used; analytical and Monte Carlo methods. A study by Newhauser *et al* [6] showed a better agreement between Monte Carlo calculations and measurements than an analytical approach, and it is estimated that the cost of over shielding due to inaccurate shielding calculations can be up to 2 m USD [2].

It is essential that an overall safety system, including personnel protection system, is in place. Like in conventional radiotherapy, this will ensure that no beam is given in the treatment area when personnel is present. Furthermore, this system will make sure beam stop devices are inserted into the beamline if there are any error conditions detected, for example, when the doors to a treatment area are opened.

In addition to possible exposure from secondary radiation, personnel can get radiation exposure from activated materials. The patient will be activated after the treatment, this entails mostly short-lived nuclides like ^{11}C ($T_{1/2}$ 20 min), with a total expected activity of up to 25 MBq per patient [7]. For occupational exposure the handling of components such as range shifters and especially apertures might be a more concerning factor. Apertures are usually made out of brass, and when hit with a high energy proton beam, activation products like ^{54}Mn ($T_{1/2}$ 312.2 d) and ^{67}Ga ($T_{1/2}$ 78.3 h) are generated [8]. As these apertures are patient specific, personnel could be handling these several times a day. Mukherjee [9] found a reduction of extremity doses for personnel of 50 % when allowing the apertures to decay for 15 minutes. Therefore, in addition to shielding and safety systems, standard operating procedures should be in place to further reduce personnel exposure.

Conclusion

An overview of important radiation safety related aspects of proton therapy was provided, including the pathways of possible personnel exposure and mitigation of these risks.

References

[1] Radhe Mohan, David Grosshans, Proton therapy – Present and future, Advanced Drug Delivery Reviews 2017, 109:26-44

[2] Newhauser, W. D., & Zhang, R. The physics of proton therapy. Physics in Medicine and Biology 2015, 60(8): 155–209.

[3] ICRP. Ann ICRP. The 2007 Recommendations of the International Commission on Radiological Protection. ICRP publication 2007, 103: 1–332

[4] IAEA. Radiological Safety Aspects of the Operation of Proton Accelerators. Vienna, Austria: 1988

[5] Daartz *et al*. Radiation safety for pregnant staff in proton therapy centers. PTCOG 52

[6] Newhauser WD, Titt U, Dexheimer D, Yan X, Nill S. Neutron shielding verification measurements and simulations for a 235-MeV proton therapy center. Nucl Instrum Meth A. 2002, 476:80–4.

[7] Qaim S.M., Activation Products in Proton Therapy, Lecture delivered during the Workshop on Nuclear Data for Medical Applications, Abdus Salam ICTP, Trieste, Italy, 12 to 23 November 2007

[8] M. Faßbender, Yu.N. Shubin, V.P. Lunev, S.M. Qaim, Experimental studies and nuclear model calculations on the formation of radioactive products in interactions of medium energy protons with copper, zinc and brass: Estimation of collimator activation in proton therapy facilities, Applied Radiation and Isotopes 1997, 48(9):1221–1230

[9] Mukherjee B. Radiation safety issues relevant to proton therapy and radioisotope production medical cyclotrons. Radiat Prot Environ 2012, 35:126-3